(2)

MTL TR 88-44

AD

AD-A205 431

ASSESSING HYDROGEN ASSISTED CRACKING MODES IN HIGH STRENGTH STEEL WELDS

STEVEN A. GEDEON
MATERIALS PRODUCIBILITY BRANCH
U.S. ARMY MATERIALS TECHNOLOGY LABORATORY

THOMAS W. EAGAR
MASSACHUSETTS INSTITUTE OF TECHNOLOGY

December 1988

Approved for public release; distribution unlimited.

US ARMY
LABORATORY COMMAND
MATERIALS TECHNOLOGY LABORATORY

U.S. ARMY MATERIALS TECHNOLOGY LABORATORY
Watertown, Massachusetts 02172-0001

The findings in this report are not to be construed as an official Department of the Army position, unless so designated by other authorized documents.

Mention of any trade names or manufacturers in this report shall not be construed as advertising nor as an official indorsement or approval of such products or companies by the United States Government.

DISPOSITION INSTRUCTIONS

Destroy this report when it is no longer needed.
Do not return it to the originator.

UNCLASSIFIED

SECURITY CLASSIFICATION OF THIS PAGE (When Data Entered)

REPORT DOCUMENTATION PAGE		READ INSTRUCTIONS BEFORE COMPLETING FORM
1. REPORT NUMBER MTL TR 88-44	2. GOVT ACCESSION NO.	3. RECIPIENT'S CATALOG NUMBER
4. TITLE (and Subtitle) ASSESSING HYDROGEN ASSISTED CRACKING MODES IN HIGH STRENGTH STEEL WELDS		5. TYPE OF REPORT & PERIOD COVERED Final Report 6. PERFORMING ORG. REPORT NUMBER
7. AUTHOR(s) Steven A. Gedeon and Thomas W. Eagar		8. CONTRACT OR GRANT NUMBER(s)
9. PERFORMING ORGANIZATION NAME AND ADDRESS U.S. Army Materials Technology Laboratory Watertown, Massachusetts 02172-0001 ATTN: SLCMT-MEM		10. PROGRAM ELEMENT, PROJECT, TASK AREA & WORK UNIT NUMBERS D/A Project: 1L162105.AH84 AMCMS Code: 612105.H84
11. CONTROLLING OFFICE NAME AND ADDRESS U.S. Army Laboratory Command 2800 Powder Mill Road Adelphi, Maryland 20783-1145		12. REPORT DATE December 1988 13. NUMBER OF PAGES 13
14. MONITORING AGENCY NAME & ADDRESS(if different from Controlling Office)		15. SECURITY CLASS. (of this report) Unclassified 15a. DECLASSIFICATION/DOWNGRADING SCHEDULE

16. DISTRIBUTION STATEMENT (of this Report)

Approved for public release; distribution unlimited.

17. DISTRIBUTION STATEMENT (of the abstract entered in Block 20, if different from Report)

18. SUPPLEMENTARY NOTES

Steven A. Gedeon is Welding Engineer, U.S. Army Materials Technology Laboratory, Watertown, MA 02172-0001. Thomas W. Eagar is Professor, Massachusetts Institute of Technology, Cambridge, MA 02139.

19. KEY WORDS (Continue on reverse side if necessary and identify by block number)

High strength steel
Welding
Implant tests
Hydrogen embrittlement
Cracking (fracturing)
Stress intensity

20. ABSTRACT (Continue on reverse side if necessary and identify by block number)

(SEE REVERSE SIDE)

DD FORM 1 JAN 73 1473 EDITION OF 1 NOV 65 IS OBSOLETE

UNCLASSIFIED

SECURITY CLASSIFICATION OF THIS PAGE (When Data Entered)

Block No. 20

ABSTRACT

The stress intensity which causes crack propagation in high strength steel weldments was quantified as a function of the hydrogen content at the crack location. This relationship was used to assess previously proposed theoretical hydrogen assisted cracking mechanisms. It was found that the microplasticity theory of Beachem can best describe how the stress intensity factor and hydrogen content affect the modes of intergranular, quasi-cleavage, and microvoid coalescence fracture.

Implant test results were analyzed with the aid of fracture mechanics to determine the stress intensity associated with various modes of fracture. Diffusible weld hydrogen results were analyzed with the aid of a hydrogen distribution model developed by Coe and Chano to determine the amount of hydrogen present at the crack location at the time of fracture.

The stress intensity and hydrogen content responsible for the microvoid coalescence fracture mode have been quantified for the high strength steel used in this study. The resulting relationship agrees with the results of Beachem but extend his theory to a wider range of hydrogen contents.

CONTENTS

Page

INTRODUCTION 1

Hydrogen Assisted Cracking Mechanism Theories 1
Quantification of the Stress Intensity in a Weld 2
Determination of Hydrogen Content in the Cracking Zone 2

EXPERIMENTAL PROCEDURE 3

EXPERIMENTAL RESULTS 4

DISCUSSION 9

SUMMARY 10

ACKNOWLEDGMENTS 10

REFERENCES 11

INTRODUCTION

It is known that hydrogen assisted cracking is a complex function of the amount of hydrogen, the stress, the temperature, and the microstructure of the steel. The purpose of this study is to quantify the amount of hydrogen which causes crack propagation as a function of stress intensity for a specific material and temperature. This relationship is then compared to existing cracking mechanism theories.

Previous literature concerning cracking theories, stress intensity determination, and hydrogen content determination is briefly reviewed.

Hydrogen Assisted Cracking Mechanism Theories

The results of theoretical studies of hydrogen embrittlement mechanisms proposed by physical metallurgists have rarely been applied to the field of welding. Sawhill's study of HY-130 steel weldments,[1] however, provides a good background for the ensuing analysis of the most often proposed hydrogen embrittlement mechanisms. Even though the problem of hydrogen embrittlement has been studied extensively, no one theory has become generally accepted.

The planar pressure theory, proposed by Zapffee, is based on the decrease in solubility of hydrogen as the temperature is lowered.[2] The atomic hydrogen is postulated to reassociate into diatomic hydrogen in pores and microvoids. The pressure of diatomic hydrogen then builds to very high values which adds to the applied external stresses. By applying Sievert's law, it is estimated that a steel with 5 ppm hydrogen would have over 17,000 atmospheres pressure in the voids at 20° C. However, several experimental observations conflict with this mechanism. Hydrogen embrittlement can be eliminated by degassing even after exposure to room temperature. The low temperature of the degassing would not be high enough to dissociate the diatomic hydrogen into monatomic hydrogen which could diffuse out of the steel. Also, the observation of hydrogen induced cracks growing on a free surface precludes an internal pressure gradient as the driving force for crack growth.

The adsorption theory of Petch and Stables[3] and further modifications[4] propose a lowering of the surface free energy by hydrogen so that a crack can grow under a lower applied stress. This theory has been criticized on the basis that the small but finite plastic deformation observed on hydrogen induced fracture surfaces requires more energy than could be explained by the adsorption theory. In addition, fracture surfaces indicate rapid void formation and coalescence at low temperatures where the rate of surface migration would be negligible.

A theory proposed by Troiano[5] suggests that hydrogen interacts with dislocation pileups in areas of triaxial stress to lower the cohesive strength. It is known that hydrogen will diffuse toward regions of high triaxial stress such as those associated with a stress riser. When the concentration reaches a given level, the interaction of hydrogen with dislocation arrays ahead of the stress riser is postulated to be sufficient to cause fracture. Troiano suggests that this interaction is due to the valence electrons from hydrogen atoms entering the unfilled "d" shells of the iron and modifying the repulsive forces which determine the interatomic spacing in transition metals.

Others have modified the planar pressure theory and the adsorption theory by assuming that hydrogen atoms are transported to the void or crack tip as Cottrell atmospheres. Bastein has proposed that hydrogen atoms are carried along by the movement of dislocations during plastic deformation. Thus, he reasons, dislocation pileups at structural defects will produce an oversaturation of hydrogen which will result in an increase in pressure which in turn produces triaxial stresses and embrittlement.[6] Research by Graville supports the hypothesis that hydrogen transport by dislocations to the site of crack initiation is a necessary part of the embrittlement process.[7,8]

Beachem has proposed a theory of hydrogen assisted cracking which is based on a microplasticity mechanism rather than embrittlement.[9] He suggests that the hydrogen in the lattice ahead of the crack tip assists whatever microscopic deformation processes the microstructure will allow. Thus, intergranular, quasi-cleavage, or microvoid coalescence fracture modes will operate depending on the microstructure, the crack tip stress intensity, and the concentration of hydrogen. The model unifies several theories but shows that the planar pressure and adsorption theories are unnecessary. He proposes that the basic hydrogen-steel interaction appears to be an easing of dislocation motion or generation, or both.

In all of the above studies, the specimen was charged with hydrogen in order to examine the effect on fracture. However, Bonisewski and Moreton[10] have observed that hydrogen introduced by this means will not behave in the same way as does that introduced by an actual welding process.

Quantification of the Stress Intensity in a Weld

Among the various testing methods for assessing hydrogen embrittlement, the implant test has become one of the most popular for scientific investigations of the cracking phenomenon in welds. This is due to the fact that the stress, hydrogen level, and microstructure can be independently varied and controlled. Crack susceptibility using this test is typically defined as the lower critical stress (LCS). The LCS is the maximum stress at which fracture does not occur for an arbitrarily long period of time (usually 1 to 3 days).

Fracture mechanics can be used to determine the stress intensity associated with fracture in the implant specimens. Since the helical notch used on the implant specimens is too blunt to use linear elastic fracture mechanics (LEFM), the crack initiation process is difficult to quantify. However, once hydrogen embrittlement occurs, the embrittled region itself will act as a sharp crack tip, and one can use LEFM to investigate the fracture of the remaining area, at least in high strength welds.

Daoud, et al., have determined the stress concentration factor for an edge cracked circular bar in tension, and have since modified this to include the effect of the crack geometry.[11,12] Even though their analysis does not include the effect of a restraining weld close to the crack, it can be used to give an approximation of the K_IC of the final fractured area.

Scanning electron microscopy (SEM) of the fractured implant specimens can be used to determine the crack geometry. Specimens with the same crack geometry as that studied by Daoud, et al., can then be used to determine the stress intensity factor associated with that fracture.

Determination of Hydrogen Content in the Cracking Zone

The diffusible hydrogen test can be used to determine the amount of hydrogen initially solidified into the weld pool. However, since fracture in the implant specimens will occur some time after the weld has cooled down, and some hydrogen will have been lost by diffusion, these results must be analyzed to determine the amount of hydrogen remaining in the cracking zone at the instant of fracture.

The amount and distribution of hydrogen remaining in an implant specimen as a function of time after welding can be estimated with the aid of a model initially developed by Coe and Chano.[13] They used an iterative procedure using small time-at-temperature increments to calculate the effect of time on the hydrogen distribution. The results are presented as hydrogen as a function of the nondimensional parameter τ. This value is defined as:

$$\tau = D\,t / l_0^2 \qquad (1)$$

where D is the diffusivity of hydrogen in solid iron, t is time, and l_0 is the weld bead depth. A sample of their distribution plots is shown in Figure 1 which shows the hydrogen distribution as a function of distance in the weld for various values of τ. A better plot for the purposes of this research is shown in Figure 2 which shows the hydrogen concentration as a function of τ at various weld locations.

It has been postulated that dislocation sweeping will increase the actual amount of hydrogen at the crack tip. The increased solubility of hydrogen under an applied axial tensile stress has been estimated to be 5 times higher than the nominal solubility by Louthan, et al.[14] Andersson[15] used a finite element technique to estimate that the hydrogen in front of a crack tip is about 1.2 times the nominal bulk hydrogen value. Schulte and Adler,[16] using nuclear reaction analysis of deuterium distribution, determined that the maximum hydrogen will be about 1.4 times the nominal bulk hydrogen concentration.

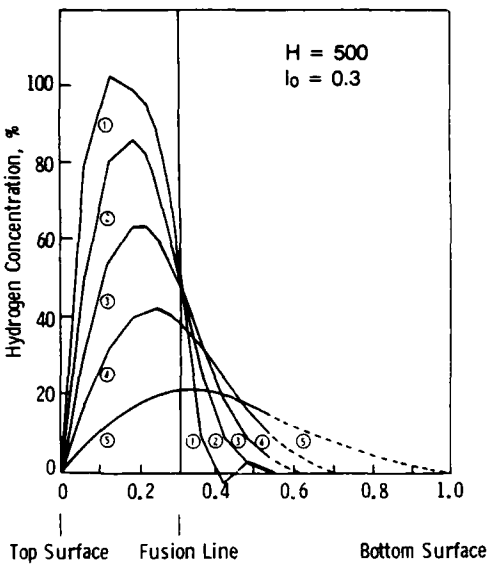

Figure 1. Hydrogen distribution as a function of distance in the weld for τ = 0.011, 0.044, 0.10, 0.20, and 0.50 (Ref. 13).

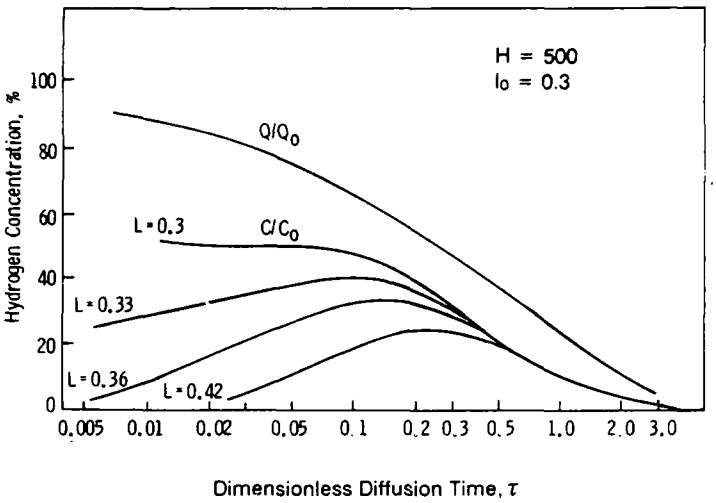

Figure 2. Hydrogen concentration as a function of τ for different locations in the weld. C_0 is the amount of hydrogen initially in the weld, and Q is the total amount in the weld region (Ref. 13).

EXPERIMENTAL PROCEDURE

Although no standard procedure exists for the implant method,[17] the IIW has published a document[18] containing guidelines for performing this test. These procedures were followed in this study using the I65 notch geometry and a helical notch.

A loading time of 5 minutes was chosen based on previous research by Peng[19] who showed that variations in loading time from 2 to 7 minutes after welding did not affect the lower critical stress (LCS). A 24-hour loading time was also chosen so that the hydrogen distribution model of Coe and Chano[13] could be used to determine the amount of hydrogen in the cracking zone.

The material studied in this investigation is a high strength steel conforming to MIL-A-46100C.[20] Its main use is for armor in military applications and it is the main structural steel used in the M1 tank. Chemical composition requirements in MIL-A-46100C are very broad as the main performance criteria are good hardenability and ballistic integrity. Due to its extremely high hardness, this material is very susceptible to hydrogen embrittlement.

The composition of the 46100 steel used throughout this investigation is listed in Table 1. It is composed primarily of tempered martensite with some banding. Due to the high hardness (HRC 53), this steel had to be normalized to HRC 35 in order to be machined into implant specimens. The specimens were then austenitized in vacuum, quenched in oil, and tempered in air to their original condition. The implant specimens were machined longitudinal to the rolling direction.

Table 1. COMPOSITION OF THE STEEL USED IN THIS STUDY

	C	Si	Mn	Cu	P	Ni	S	Al	Cr	Mo
MIL-A-46100	0.31	0.41	0.97	0.38	0.011	1.21	0.008	0.044	0.51	0.50

Diffusible hydrogen testing was performed in accordance with AWS A4.3-86. The Gas Chromatography method was used with a Yanaco hydrogen analyzer model G-1006.

By varying the amount of hydrogen in the GMAW shielding gas, time to loading, and preheat temperature, the amount of hydrogen remaining in the weldment at the time of cracking can be varied. A matrix of seven conditions was studied for each shielding gas composition:

1. diffusible weld hydrogen content (as per AWS A4.3-86);
2. hydrogen remaining 24 hours after welding (the AWS specimen was allowed to cool for 24 hours before being analyzed);
3. hydrogen remaining 24 hours after welding with preheat;
4. LCS when loaded 5 minutes after welding;
5. LCS when loaded 24 hours after welding;
6. LCS when loaded 5 minutes after welding with preheat; and
7. LCS when loaded 24 hours after welding with preheat.

Seven different shielding gas compositions were studied although not every gas was evaluated both with and without preheat.

A scanning electron microscope (SEM) was used to examine the fractured surfaces of the implant specimens. The initial fracture in the majority of specimens was due to hydrogen embrittlement, with the remaining area failing due to microvoid coalescence. Quantitative fractography was performed to map the various failure zones across the failed surfaces of over 60 implant specimens.

EXPERIMENTAL RESULTS

Table 2 summarizes the experimental results acquired in this portion of the research program. Each LCS value was determined from a plot of time-to-fracture versus applied stress. Two such plots show the effect of preheat (Figure 3) and hydrogen in the shielding gas (Figure 4).

Table 2. SUMMARY OF EXPIRIMENTAL RESULTS

%H_2 Added to Shield Gas	%O2 Added to Shield Gas	Preheat	LCS 5 min	LCS 24 hr	H 3 sec	H 24 hr
0	2	None	48.5	58	2.14	0.74
0	2	150°F	79	–	–	0.29
0	2	250°F	82.5	86	–	0.22
0.01	2	None	56	52.5	4.52	1.09
0.1	2	None	46	48.5	6.80	1.23
0.1	2	250°F	47.5	52	–	0.42
0.5	2	None	28	39	8.28	1.96
0.5	1	None	–	–	8.42	1.80
0.5	1	250°F	45	53	–	1.58
2	2	None	25	–	14.0	–
2	1	None	26.5	34	8.17	2.19
2	1	250°F	45	–	–	1.31

The ratio Q/Q_o in Figure 2 is approximately equal to the ratio of the hydrogen content at 24 hours divided by the initial hydrogen content. Using the data from Table 2, this ratio averages 0.25 for welds made without preheat. From Figure 2, this corresponds to a τ of 0.9, which is very close to the value of 1.0 found if τ is calculated directly from the cooling curve and diffusivity versus temperature data.

Based on the experimentally determined τ value of 0.9, the amount of hydrogen located at the fusion line ($l = l_0 = 0.3$ in Figure 2) will be equal to 12.5% of the initial hydrogen content in the weld. For welds made with 250°F preheat, Q/Q_o averages 0.13 twenty-four hours after welding which corresponds to a τ of 1.9.

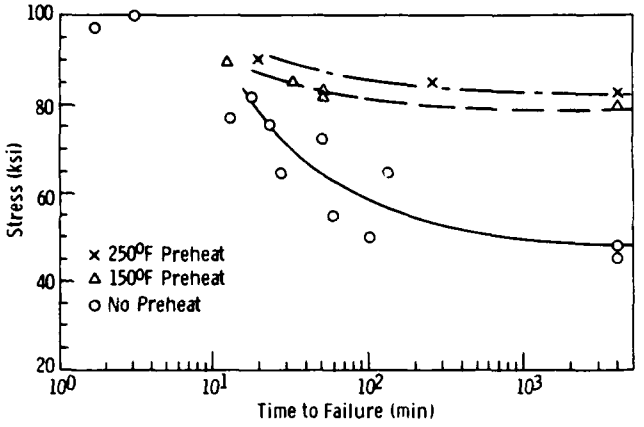

Figure 3. Implant test results for GMA welds made with 0% H_2 / 2% O_2 / Ar and loaded 5 minutes after welding. Curves depict welds made with 250°F, 150°F, and no preheat.

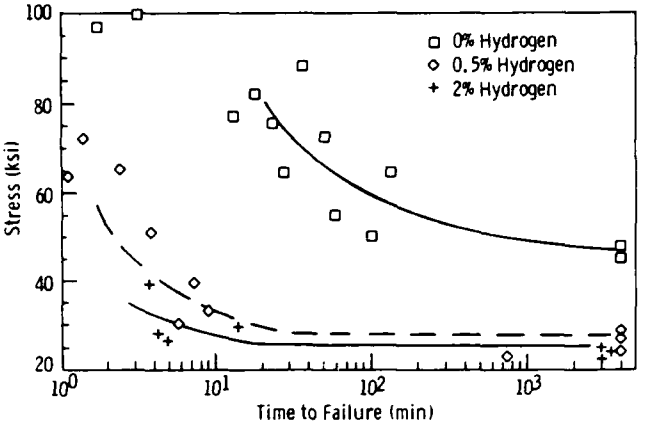

Figure 4. Implant test results for GMA welds made with 2% O_2 and loaded after 5 minutes. Curves depict 0%, 0.5%, and 2% H_2 added to the shielding gas.

In this way, the amount of hydrogen at the cracking zone during the final fracture can be found for each of the implant specimens. This amount of hydrogen is termed the bulk hydrogen in the cracking zone and does not include any increased amount which may be due to the increased stress state at the crack tip.

In order to determine the stress intensity which caused cracking, a fractographic analysis of the fractured implant specimens was performed. The cracking zone in all of the implant fractures studied was at the weld fusion line.

Figure 5 shows a typical overall view of the fractured surface of an implant specimen. Figure 6 shows the location of each of the magnified photos taken of this surface. Figure 7 shows the fracture morphology typical of hydrogen embrittlement as evidenced by intergranular faceting. The fracture morphology associated with microvoid coalescence is shown in Figure 8 as evidenced by the ductile dimples. The transition region showing areas of intergranular faceting below or next to areas of microvoid coalescence is shown in Figure 9. The resulting quantitative fracture map developed for this specimen is depicted in Figure 10.

Not all of the specimens exhibited such a clear distinction between the different fracture zones. For example, a number of the low hydrogen samples had areas of "fisheyes." A "fisheye" is an inclusion which is locally surrounded by an area of hydrogen embrittlement. The local area of hydrogen embrittlement surrounding a "fisheye" is presumed to be due to hydrogen trapping at the inclusion. Numerous investigators have found that hydrogen can be trapped at inclusions.[21-23]

Of 140 fractured implant specimens, only 60 had cracks starting from one edge. Of the fracture maps developed for these 60 specimens, the 12 which very closely approximated the crack geometry studied by Daoud, et al., were used to determine the fracture toughness (as estimated by K_{IC}) of the area which fractured due to microvoid coalescence. Table 3 gives a presentation of the results for these 12 specimens. The hydrogen values shown in Table 3 were determined by estimating τ from the cooling curve and the time at which fracture occurred, and finding the corresponding hydrogen concentration from Figure 2. The a/D ratio corresponds to the region of intergranular fracture which was assumed to approximate a crack.

The resulting plot of stress intensity versus amount of hydrogen in the cracking zone is shown in Figure 11. As can be seen, the stress intensity (an approximation of K_{IC}) at which microvoid coalescence occurs decreases with increasing hydrogen in the crack zone. However, at very high hydrogen contents, intergranular fracture will be more energetically favorable than microvoid coalescence until very high stress intensities are reached.

Figure 5. Overall SEM view of a fractured implant specimen surface, Mag. 15X.

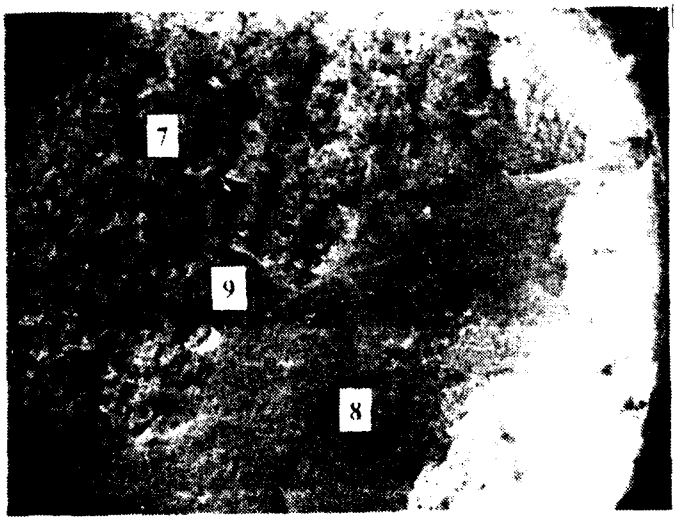

Figure 6. Schematic showing the regions from which the magnified photos were taken, Mag. 15X.

Figure 7. Region of intergranular fracture characteristic of hydrogen embrittlement, Mag. 1500X.

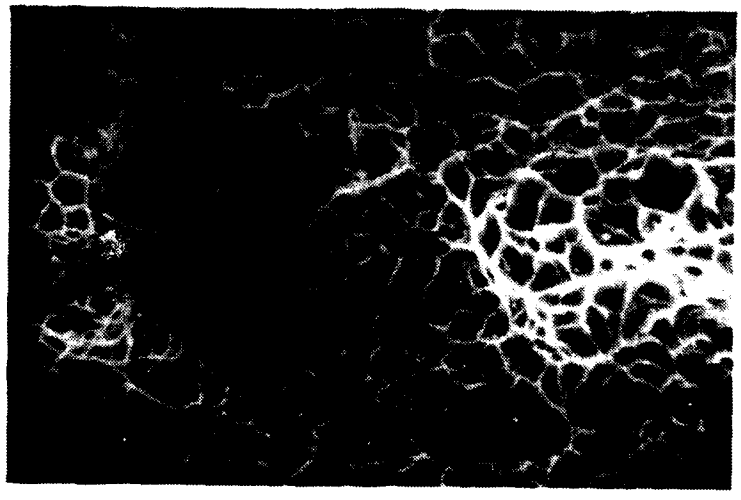

Figure 8. Region of microvoid coalescence showing ductile dimples, Mag. 1500X.

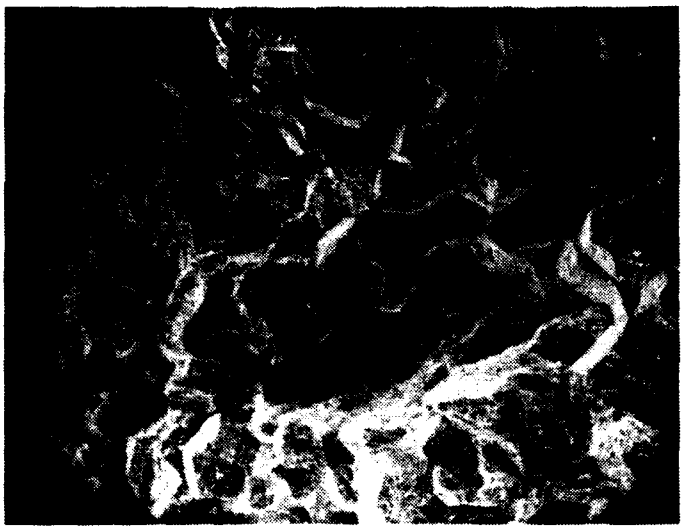

Figure 9. Transition region where both intergranular fracture and microvoid coalescence are evidenced, Mag. 150X.

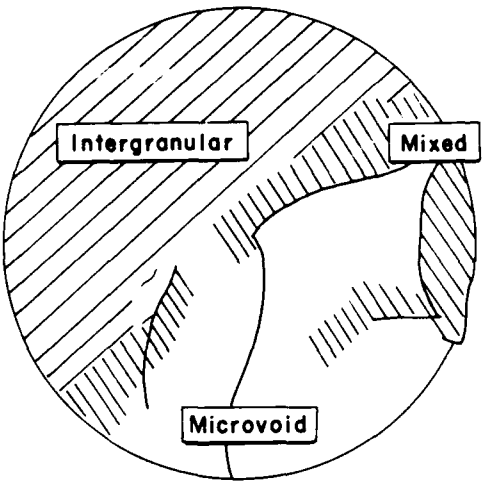

Figure 10. Quantitative fracture map showing the regions of fracture types.

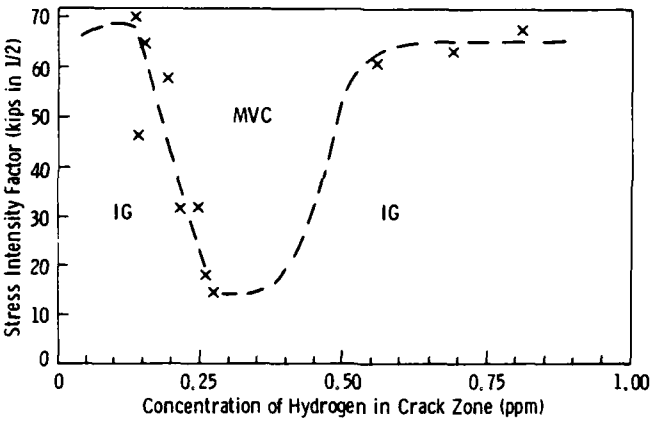

Figure 11. Interrelationship developed in this study between the stress intensity factor, hydrogen content in the cracking zone, and mode of fracture.

Table 3. TABULATION OF FRACTURE TOUGHNESS ESTIMATES

Sample	Stress (ksi)	a/D	K_IC (ksi $\sqrt{in.}^{1/2}$)	Estimated H at Crack Tip (ppm)
1.3	88.4	0.30	46.3	0.14
1.4	82.2	0.42	65.0	0.15
2.18	24.3	0.45	17.9	0.26
2.20	113.0	0.13	32.0	0.245
3.6	24.0	0.41	14.4	0.275
4.1	89.2	0.15	31.6	0.215
4.6	82.8	0.35	57.8	0.19
17.2	55.0	0.50	70.5	0.135
2.2	82.2	0.41	68	0.81
16.5	27.0	0.60	60.8	0.56
20.1	28.0	0.60	63.1	0.69

DISCUSSION

The implant specimens which were welded with a high hydrogen content in the shielding gas (2% H_2), had a K_IC of about 16 MPa $m^{1/2}$ (15 ksi $\sqrt{in.}^{1/2}$). This value agrees quite closely with the work of Herman and Campbell,[24] who used fracture toughness samples of this identical type of steel and determined the stress corrosion cracking toughness, Kscc. Herman and Campbell found that the fracture toughness of this material was 16 MPa $m^{1/2}$ (15 ksi $\sqrt{in.}^{1/2}$) when exposed to distilled water.

At low hydrogen levels (0% H_2 added to the shielding gas), the final fractures had a toughness of approximately 71 MPa $m^{1/2}$ (65 ksi $\sqrt{in.}^{1/2}$), which is the same value found by Herman and Campbell[24] for the fracture toughness of samples not exposed to a corrosive environment. This datum point has been plotted in Figure 11 for the K_IC associated with hydrogen free specimens.

At medium levels of hydrogen (0.5% H_2 added to the shielding gas), the K_IC varied with the applied load and time to failure. At low applied loads, the fracture toughness was almost as low as the Kscc value. At higher loads, the value increased to approximately the nominal K_IC value of 71 MPa $m^{1/2}$ (65 ksi $\sqrt{in.}^{1/2}$). In a few cases, very small amounts of hydrogen seemed to increase the K_IC of microvoid coalescence fracture above the K_IC of hydrogen free specimens. Hydrogen induced strengthening has been documented by others.[14] White[25] also noticed some slight strengthening of her implant specimens when welding with 0.05% hydrogen in the shielding gas. This phenomenon may be due to hydrogen pinning the dislocations.

There were a number of specimens which had both high hydrogen contents and high K_IC values. These hydrogen values were much higher than in specimens with K_IC values of 16 MPa $m^{1/2}$ (15 ksi $\sqrt{in.}^{1/2}$). With the exception of the three points at very high hydrogen contents, the relationship determined in this investigation quantifies the theoretical fracture mechanism initially proposed by Beachem.[9]

One of the main features of the Beachem theory is the classification of fracture modes with respect to stress and hydrogen level. At relatively high stresses, hydrogen assisted cracking can propagate by microvoid coalescence, which is normally thought of as a ductile failure mechanism. Beachem proved that hydrogen can be responsible for microvoid coalescence by partially fracturing a sample in hydrogen, then freezing the sample in liquid nitrogen and sectioning the sample to find evidence of the processes occurring ahead of the crack tip. As the stress intensity decreases, crack propagation proceeds by the lower plastic deformation processes of quasi-cleavage, and finally, intergranular separation. Increasing hydrogen concentration at the crack tip has the effect of decreasing the stress intensity at which these fracture processes occur.

Beachem's model adequately explains the presence of plastic deformation preceding hydrogen cracking in the HAZ of welds[26] and plastic deformation in other systems as well.[27-29] Also, the qualitative experimental results postulated by Beachem in Figure 12 bear a remarkable resemblance to the quantitative results of the present investigation.

The major difference between the fracture map proposed by Beachem and the one found in the present investigation, is that this investigation shows that intergranular failure can still occur at much higher values of hydrogen. It makes sense that intergranular failure will occur at high hydrogen contents, but Beachem suggests that microvoid coalescence will occur faster, and thus predominate. The three points at high hydrogen concentrations are beyond the range investigated by Beachem. Thus, Figure 11 shows a modification to the original work by Beachem, namely, that high hydrogen concentrations can suppress the microvoid coalescence fracture mode, and that intergranular fracture will still be operative. The Beachem model appears to be the most comprehensive model to date, and accounts for most experimental observations of hydrogen cracking.

The present investigation did not quantify the hydrogen concentration which caused intergranular or quasi-cleavage fracture. There were not enough specimens which exhibited the proper amount of quasi-cleavage fracture along with a crack geometry which approximated the fracture mechanical analysis of Daoud, et al.

An attempt was made to quantify the relationship between stress intensity and hydrogen content for which no hydrogen assisted cracks will propagate. In an unfractured specimen, it is assumed that a very small crack exists for which a/D is less than 0.2. From Daoud, et al., the stress intensity factor will be approximately unity. In this case, the maximum hydrogen present in the lower critical stress specimens can be used along with the applied stress (the LCS

value) and the assumed a/D ratio to develop the "no hydrogen assisted cracking" region in Figure 13. This region should be considered tentative at the present time since the assumptions are not necessarily justified.

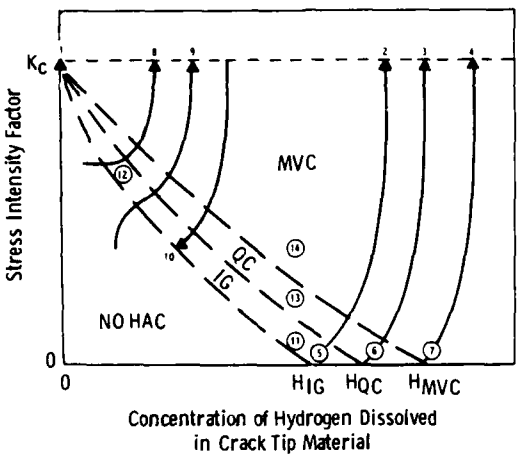

Figure 12. Suggested interrelationship by Beachem between stress intensity factor, dissolved hydrogen content, and HAC deformation mode of microscopically small volumes of crack tip material. (Ref. 9)

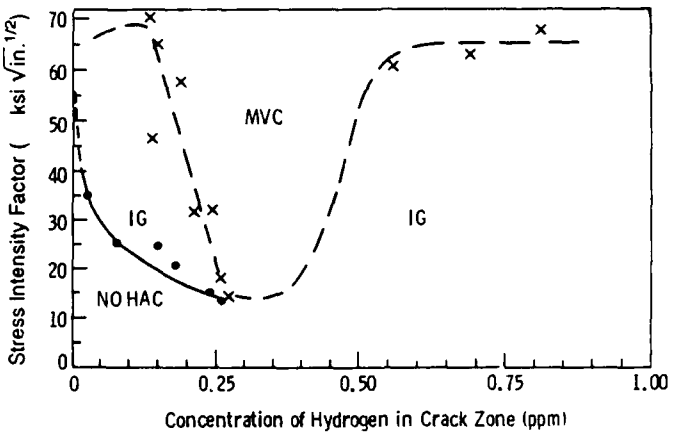

Figure 13. Interrelationship between the stress intensity factor, hydrogen content, and mode of fracture, including a hypothesized no cracking region.

The current research has attempted to quantify both the stress intensity factor and the amount of hydrogen responsible for causing microvoid coalescence. This is the first time that this has been attempted. Discrepancies may arise due to the fact that the implant specimens were not well suited to K_{IC} measurements. Another shortcoming may be that the bulk hydrogen in the cracking zone was determined rather than the hydrogen due to dislocation sweeping or stress concentrations at the crack tip. However, the relationships developed in this investigation may be accurate since the increased amount of hydrogen due to stress concentrations may be only a factor of about 1.4.

Hopefully, future research will enable anticipated hydrogen levels to be used to quantify the allowable defect size which will result in a stress intensity factor lower than that which causes hydrogen assisted cracking. Thus, very low hydrogen welds can be designed to either allow higher stresses or larger defects than high hydrogen welds.

SUMMARY

The fracture mode of high strength steel welds has been characterized as a function of the stress intensity and hydrogen content at the cracking zone in implant tested welds. The results indicate that the hydrogen embrittlement theory originally proposed by Beachem can be used to explain the effect of hydrogen on cracking of high strength steels. The results of the present study increase the range of hydrogen above that used in the original Beachem study to show that large amounts of hydrogen will increase the propensity for intergranular fracture rather than microvoid coalescence.

This method of analyzing hydrogen fracture shows some promise for choosing acceptable flaw sizes based on the anticipated amount of hydrogen. The flaw size must be chosen such that the resulting stress intensity will not cause hydrogen cracking at the anticipated hydrogen level.

ACKNOWLEDGMENTS

The authors wish to express their gratitude to the U.S. Army Materials Technology Laboratory for financial support of this project. In addition, portions of this work performed at M.I.T. and were supported by the Office of Naval Research under contract N00014-80-C-0384. Also, the competent assistance of James Catalano and Atillio Santoro are gratefully acknowledged.

REFERENCES

1. SAWHILL, J.M. Jr. *A Modified Implant Test for Studying Delayed Cracking.* Ph.D. dissertation, Rensselaer Polytechnic Institute, Troy, NY, 1973.
2. ZAPFFE, C.A., and SIMS, C.E. *Hydrogen Embrittlement, Internal Stress, and Defects in Steel.* Trans. AIME, v. 145, 1941, p. 225-259.
3. PETCH, N.O., and STABLES, P. *Delayed Fracture of Metals Under Static Load.* Nature, v. 169, 1952, p. 842-843.
4. PETCH, N.O. *Lowering of the Fracture Stress Due to Surface Adsorption.* Philosophical Magazine, Series 8, v. 1, 1956, p. 331-335.
5. TROIANO, A.R. *The Influence of Hydrogen on the Mechanical Behavior of Steel.* Special Report No. 73, The Iron and Steel Institute, 1962.
6. BASTIEN, P. and AZOU, P. *Effect of Hydrogen on the Deformation and Fracture of Iron and Steel in Simple Tension.* Proc. First Word Metallurgical Congress, ASM, Cleveland, OH, 1951, p. 535-552.
7. GRAVILLE, B.A. *Effect of Hydrogen Concentration on Hydrogen Embrittlement.* British Welding Journal, v. 15, no. 4, 1968, p. 191-195.
8. GRAVILLE, B.A., BAKER, R.G., and WATKINSON, F. *Effect of Temperature and Strain Rate on Hydrogen Embrittlement of Steel.* British Welding Journal, v. 14, no. 6, 1967, p. 337-342.
9. BEACHEM, C.D. *A New Model for Hydrogen Assisted Cracking (Hydrogen Embrittlement).* Metallurgical Transactions, v. 3, no. 2, 1972, p. 437-451.
10. BONISZEWSKI, T., and MORETON, J. *Hydrogen Entrappment in Mild Steel Weld Metal with Micropores.* Metal Construction, v. 1, no. 6, 1969, p. 269-276.
11. DAOUD, O.E.K., and CARTWRIGHT, D.J. *Strain Energy Release Rate for a Circular-Arc Edge Crack in a Bar Under Tension or Bending.* Journal of Strain Analysis, v. 20, no. 1, 1985, p. 53-58.
12. DAOUD, O.E.K., CARTWRIGHT, D.J., and CARNEY, M. *Strain Energy Release Rate for a Single-Edge-Cracked Circular Bar in Tension.* Journal of Strain Analysis, v. 13, no. 2, 1978, p. 83-89.
13. COE, F.R., and CHANO, Z. *Hydrogen Distribution and Removal for a Single Bead Weld During Cooling.* Welding Research Institute, v. 5, 1975, p. 33-90.
14. LOUTHAN, M.R., MCNITT, R.P., and SISSON, R.D. *Importance of Stress State on Hydrogen Embrittlement.* Advanced Techniques for Characterizing Hydrogen in Metals, N.F. Fiore, and B.J. Berkowitz, ed., The Metallurgical Society of AIME, NY, 1982, p. 25-42.
15. ANDERSSON, B. *Hydrogen Cracking in Weldments.* Ph.D. dissertation, Gothenburg, Chalmers University of Technology, 1981.
16. SCHULTE, R.L., and ADLER, P.N. *Evaluation of Stress-Induced Hydrogen and Deuterium Redistribution in Titanium Alloys Using Nuclear Reaction Analysis.* Advanced Techniques of Characterizing Hydrogen in Metals, N.F. Fiore and B.J. Berkowitz, ed., The Metallurgical Society of AIME, 1982, p. 233-244.
17. BRYHAN, A.J. *The Effect of Testing Procedure on Implant Test Results.* Welding Journal, v. 59, no. 9, 1981, p. 169s-176s.
18. *Cold Cracking Test Methods Using Implants.* Welding in the World, v. 23 (1/2), IIS/IIW-802-84 (exdoc. IX-1240-82), 1985, p. 8-12.
19. PENG, J. *Weldability Studies of High-Strength Steels Using the Implant Test Method.* Master's Thesis, Ohio State Univeristy, Columbus, OH, 1981.
20. Military Specification, *Armor Plate, Steel, Wrought, High-Hardness.* MIL-A-46100, revision C, 1983.
21. CASKEY, G.R. Jr. *Tritium Autoradiography.* Advanced Techniques for Characterizing Hydrogen in Metals, N.F. Fiore and B.J. Berkowitz, ed., The Metallurgical Society of AIME, Warrendale, PA, 1982, p. 61-76.
22. KUMNICK, A.J., and JOHNSON, H.H. *Deep Trapping States for Hydrogen in Deformed Iron.* Acta Metallurgica, v. 28, 1980, p. 33-39.
23. TUYEN, D.L., and WILDE, B. *An Autoradiographic Technique for Studying the Segregation of Hydrogen Absorbed into Carbon and Low-Alloy Steels.* Current Solutions to Hydrogen Problems in Steel, Interrante and Pressouyre, ed., ASM, Metals Park, OH, 1982, p. 413-422.
24. HERMAN, W.A., and CAMBELL, G.M. *Environmental Assisted Cracking in High Hardness Armor Steel.* U.S. Army Materials Technology Laboratory, Technical Report TR 85-28, 1985
25. WHITE, D.R. *In Process Measurement of Hydrogen in Welding.* Ph.D. dissertation, University of Illinois, Champaign, IL, 1986.
26. HOMMA, H. *A Study of Delayed Cracking in HY-80 Weldments.* Ph.D. dissertation, Rensselaer Polytechnic Institute, Troy, NY, 1972.
27. BERNSTEIN, I.M., and PRESSOUYRE, G.M. *The Role of Traps in the Microstructure Control of Hydrogen Embrittlement of Steels.* Hydrogen Degradation of Ferrous Alloys, Oriani, Hirth, and Smialowski, ed., Noyes Publications, 1985, p. 647-685.
28. ORIANI, R.A. *A Mechanistic Theory of Hydrogen Embrittlement of Steels.* Ber. Bunsenges Phys. Chem., v. 76, 1972, p. 848-857.
29. HIRTH, J.P. *Theories Of Hydrogen Induced Cracking In Steels.* Hydrogen Degradation of Ferrous Alloys, Oriani, Hirth and Smialowski, ed., Noyes Publications, 1985.

DISTRIBUTION LIST

No. of Copies	To
1	Office of the Under Secretary of Defense for Research and Engineering, The Pentagon, Washington, DC 20301
	Commander, U.S. Army Laboratory Command, 2800 Powder Mill Road, Adelphi, MD 20783-1145
1	ATTN: AMSLC-IM-TL
	Commander, Defense Technical Information Center, Cameron Station, Building 5, 5010 Duke Street, Alexandria, VA 22304-6145
2	ATTN: DTIC-FDAC
	Metals and Ceramics Information Center, Battelle Columbus Laboratories, 505 King Avenue, Columbus, OH 43201
1	ATTN: Harold Mindlin
	Commander, Army Research Office, P.O. Box 12211, Research Triangle Park, NC 27709-2211
1	ATTN: Information Processing Office
	Commander, U.S. Army Materiel Command (AMC), 5001 Eisenhower Avenue, Alexandria, VA 22333
1	ATTN: AMCLD
	Commander, U.S. Army Materiel Systems Analysis Activity, Aberdeen Proving Ground, MD 21005
1	ATTN: AMXSY-MP, Director
	Commander, U.S. Army Missile Command, Redstone Scientific Information Center, Redstone Arsenal, AL 35898-5241
1	ATTN: AMSMI-RD-CS-R/Doc
	Commander, U.S. Army Armament, Munitions and Chemical Command, Dover, NJ 07801
2	ATTN: Technical Library
	Commander, U.S. Army Tank-Automotive Command, Warren, MI 48397-5000
1	ATTN: AMSTA-ZSK
2	AMSTA-TSL, Technical Library
1	AMSTA-RCK
	Commander, U.S. Army Foreign Science and Technology Center, 220 7th Street, N.E., Charlottesville, VA 22901
1	ATTN: Military Tech
	Director, Eustis Directorate, U.S. Army Air Mobility Research and Development Laboratory, Fort Eustis, VA 23604
1	ATTN: SAVDL-E-MOS (AVSCOM)
1	SAVDL-EU-TAP
	U.S. Army Aviation Training Library, Fort Rucker, AL 36360
1	ATTN: Building 5906--5907
	Commander, U.S. Army Aviation Systems Command, 4300 Goodfellow Boulevard, St. Louis, MO 63120
1	ATTN: AMDAV-EGX
1	AMDAV-EX, Mr. R. Lewis
1	AMDAV-EQ, Mr. Crawford
2	AMCPM-AAH-TM, Mr. R. Hubbard, Mr. B. J. Baskett
1	AMDAV-DS, Mr. W. McClane
	Naval Research Laboratory, Washington, DC 20375
1	ATTN: Code 5830
1	Code 2627

No. of Copies	To
	Chief of Naval Research, Arlington, VA 22217
1	ATTN: Code 471
	Director, Structural Mechanics Research, Office of Naval Research, 800 North Quincy Street, Arlington, VA 22203
1	ATTN: Dr. M. Perrone
1	Edward J. Morrissey, AFWAL/MLTE, Wright Patterson Air Force Base, OH 45433
	Commander, U.S. Air Force Wright Aeronautical Laboratories, Wright-Patterson Air Force Base, OH 45433
1	ATTN: AFWAL/MLC
1	AFWAL/MLLP, D. M. Forney, Jr.
1	AFWAL/MLBC, Mr. Stanley Schulman
1	AFWAL/MLXE, A. Olevitch
	National Aeronautics and Space Administration, Marshall Space Flight Center, Huntsville, AL 35812
1	ATTN: R. J. Schwinghammer, EH01, Dir, M&P Lab
1	Mr. W. A. Wilson, EH41, Bldg. 4612
	Chief of Naval Research, Washington, DC 20350
1	ATTN: OP-987, Director
	Aeronautical Systems Division (AFSC), Wright-Patterson Air Force Base, OH 45433
1	ATTN: ASD/ENFEF, D. C. Wight
1	ASD/ENFTV, D. J. Wallick
1	ASD/XRHD, G. B. Bennett
	Air Force Armament Laboratory, Eglin Air Force Base, FL 32542
1	ATTN: AFATL/DLYA, V. D. Thornton
	Air Force Flight Dynamics Laboratory, Wright-Patterson Air Force Base, OH 45433
1	ATTN: AFFDL/FIES, J. Sparks
1	AFFDL/FIES, J. Hodges
1	AFFDL/TST, Library
	Air Force Test and Evaluation Center, Kirtland Air Force Base, NM 87115
1	ATTN: AFTEC-JT
	NASA - Ames Research Center, Army Air Mobility Research and Development Laboratory, Mail Stop 207-5, Moffett Field, CA 94035
1	ATTN: SAVDL-AS-X, F. H. Immen
	NASA - Johnson Spacecraft Center, Houston, TX 77058
1	ATTN: JM6
1	ES-5
	Naval Air Development Center, Warminster, PA 18974
1	ATTN: Code 063
1	Code 6062
	Naval Air System Command, Department of the Navy, Washington, DC 20360
1	ATTN: AIR-03PAF
1	AIR-5203
1	AIR-5164J
1	AIR-530313
	Naval Post Graduate School, Monterey, CA 93948
1	ATTN: Code 578P, R. E. Ball

No. of Copies	To
	Naval Surface Weapons Center, Dahlgren Laboratory, Dahlgren, VA 22448
1	ATTN: Code G-54, Mr. J. Hall
1	Code G-54, Dr. B. Smith
	Commander, Rock Island Arsenal, Rock Island, IL 61299
1	ATTN: AMSAR-PPV
	Armament Systems, Inc., 712-F North Valley, Anaheim, CA 92801
1	ATTN: J. Musch
	Beech Aircraft Corporation, 9709 E. Central Avenue, Wichita, KS 67206
1	ATTN: Engineering Library
	Bell Helicopter Company, A Textron Company, P.O. Box 482, Fort Worth, TX 76101
1	ATTN: J. R. Johnson
	Boeing Vertol Company, A Division of the Boeing Company, P.O. Box 16858, Philadelphia, Philadelphia, PA 19142
1	ATTN: J. E. Gonsalves, M/S P32-19
1	Cessna Military, P.O. Box 7704, Wichita, KS 67277-7704
	Fairchild Industries, Inc., Fairchild Republic Company, Conklin Street, Farmingdale, Long Island, NY 11735
1	ATTN: Engineering Library, G. A. Mauter
	FMC Corporation, Central Engineering Labs, 1185 Coleman Avenue, Box 80, Santa Clara, CA 95052
1	ATTN: Gary L. Boerman
	FMC Corporation, Ordnance Division, 1105 Coleman Avenue, Box 1201, San Jose, CA 95108
1	ATTN: William H. Altergott
	General Dynamics Corporation, Convair Division, P.O. Box 80877, San Diego, CA 92138
1	ATTN: Research Library
	Gruman Aerospace Corporation, South Oyster Bay Road, Bethpage, NY 11714
1	ATTN: Technical Information Center, J. Davis
	McDonnell Douglas Helicopter Co., 5000 East McDoweell Road Mesa, AZ 85205-9797
1	ATTN: Library
1	Mr. A. Hirko
1	Mr. L. Soffa
	IIT Research Institute, 10 West 35th Street, Chicago, IL 60616
1	ATTN: K. McKee
	Kaman Aerospace Corporation, Old Winsor Road, Bloomfield, CT 06002
1	ATTN: H. E. Showalter
	Lockheed-California Company, A Division of Lockheed Aircraft Corporation, Burbank, CA 91503
1	ATTN: Technological Information Center, 84-40, U-35, A-1
	Vought Corporation, P.O. Box 5907, Dallas, TX 75232
1	ATTN: D. M. Reedy, 2-30110
	Martin Marietta Corporation, Orlando Division, P.O. Box 5837, Orlando, FL 32805
1	ATTN: Library, M. C. Griffith

No. of Copies	To
	McDonnell Douglas Corporation, 3855 Lakewood Boulevard, Long Beach, CA 90846
1	ATTN: Technical Library, C1 290/36-84
	Northrop Corporation, Aircraft Division, 3901 W. Broadway, Hawthorne, CA 90250
1	ATTN: Mgr. Library Services, H. W. Jones
	Parker Haffifin, 14300 Alton Pkwy., Irvine, CA 92718-1814
1	ATTN: C. Beneker
	Sikorsky Aircraft, A Division of United Aircraft Corporation, Main Street, Stratford, CT 06601
1	ATTN: Mel Schwartz, Chief of Metals
	Teledyne CAE, 1330 Laskey Road, Toledo, OH 43697
1	ATTN: Librarian
	Georgia Institute of Technology, School of Mechanical Engineering, Atlanta, GA 30332
1	ATTN: Mechanical Engineering Library
	Lukens Steel Company, Coateville, PA 19320
1	ATTN: Dr. E. Hamburg
1	Mr. A. Wilson
	Republic Steel Corporation, 410 Oberlin Avenue SW, Massillon, OH 44646
1	ATTN: Mr. R. Sweeney
1	Mr. W. H. Brechtel
1	Mr. T. M. Costello
	L. Raymond Associates, P.O. Box 7925, Newport Beach CA 92658-7925
1	ATTN: Dr. L. Raymond
	Ingersoll Rand Oilfield Products Division, P.O. Box 1101, Pampa, TX 79065
1	ATTN: Mr. W. L. Hallerberg
	Brown University, Division of Engineering, Providence, RI 02912
1	ATTN: Prof. J. Duffy
	SRI International, 333 Ravenswood Avenue, Menlo Park, CA 94025
1	ATTN: Dr. D. Shockey
	Illinois Institute of Technology, Metallurgical and Materials Engineering Department, Chicago, IL 60616
1	ATTN: Dr. Norman Breyer
1	Roger Stanton, SMCAR-AET-M, Bldg. 355, Picatinny Arsenal, Dover, NJ 07806-5000
2	Dr. Jack H. Devletian, Department of Materials Science and Engineering, Oregon Graduate Center, 19600 N.W. Van Neumann Drive, Beaverton, OR 97006-1999
1	Dr. Thomas Eagar, Department of Materials Science and Engineering, MIT, Cambridge, MA 02139
1	Dr. Steven A. Gedeon, via delle industrie, 39, 30175 Porto Marghera-ve, Italy
	Director, U.S. Army Materials Technology Laboratory, Watertown, MA 02172-0001
2	ATTN: SLCMT-TML
2	Authors

U.S. Army Materials Technology Laboratory
Watertown, Massachusetts 02172-0001
ASSESSING HYDROGEN ASSISTED CRACKING MODES IN HIGH STRENGTH STEEL WELDS -
Steven A. Gedeon and Thomas W. Eagar

AD____________
UNCLASSIFIED
UNLIMITED DISTRIBUTION

Key Words

High strength steel
Welding
Implant tests

Technical Report MTL TR 88-44, December 1988, 13 pp-illus-tables, D/A Project 16162105.AH84, AMCMS Code 612105.H84

The stress intensity which causes crack propagation in high strength steel weldments was quantified as a function of the hydrogen content at the crack location. This relationship was used to assess previously proposed theoretical hydrogen assisted cracking mechanisms. It was found that the microplasticity theory of Beachem can best describe how the stress intensity factor and hydrogen content affect the modes of intergranular, quasi-cleavage, and microvoid coalescence fracture. Implant test results were analyzed with the aid of fracture mechanics to determine the stress intensity associated with various models of fracture. Diffusible weld hydrogen results were analyzed with the aid of a hydrogen distribution model developed by Coe and Chano to determine the amount of hydrogen present at the crack location at the time of fracture. The stress intensity and hydrogen content responsibile for the microvoid coalescence fracture mode have been quantified for the high strength steel used in this study. The resulting relationship agrees with the results of Beachem but extend his theory to a wider range of hydrogen contents.

U.S. Army Materials Technology Laboratory
Watertown, Massachusetts 02172-0001
ASSESSING HYDROGEN ASSISTED CRACKING MODES IN HIGH STRENGTH STEEL WELDS -
Steven A. Gedeon and Thomas W. Eagar

AD____________
UNCLASSIFIED
UNLIMITED DISTRIBUTION

Key Words

High strength steel
Welding
Implant tests

Technical Report MTL TR 88-44, December 1988, 13 pp-illus-tables, D/A Project 16162105.AH84, AMCMS Code 612105.H84

The stress intensity which causes crack propagation in high strength steel weldments was quantified as a function of the hydrogen content at the crack location. This relationship was used to assess previously proposed theoretical hydrogen assisted cracking mechanisms. It was found that the microplasticity theory of Beachem can best describe how the stress intensity factor and hydrogen content affect the modes of intergranular, quasi-cleavage, and microvoid coalescence fracture. Implant test results were analyzed with the aid of fracture mechanics to determine the stress intensity associated with various models of fracture. Diffusible weld hydrogen results were analyzed with the aid of a hydrogen distribution model developed by Coe and Chano to determine the amount of hydrogen present at the crack location at the time of fracture. The stress intensity and hydrogen content responsibile for the microvoid coalescence fracture mode have been quantified for the high strength steel used in this study. The resulting relationship agrees with the results of Beachem but extend his theory to a wider range of hydrogen contents.

U.S. Army Materials Technology Laboratory
Watertown, Massachusetts 02172-0001
ASSESSING HYDROGEN ASSISTED CRACKING MODES IN HIGH STRENGTH STEEL WELDS -
Steven A. Gedeon and Thomas W. Eagar

AD____________
UNCLASSIFIED
UNLIMITED DISTRIBUTION

Key Words

High strength steel
Welding
Implant tests

Technical Report MTL TR 88-44, December 1988, 13 pp-illus-tables, D/A Project 16162105.AH84, AMCMS Code 612105.H84

The stress intensity which causes crack propagation in high strength steel weldments was quantified as a function of the hydrogen content at the crack location. This relationship was used to assess previously proposed theoretical hydrogen assisted cracking mechanisms. It was found that the microplasticity theory of Beachem can best describe how the stress intensity factor and hydrogen content affect the modes of intergranular, quasi-cleavage, and microvoid coalescence fracture. Implant test results were analyzed with the aid of fracture mechanics to determine the stress intensity associated with various models of fracture. Diffusible weld hydrogen results were analyzed with the aid of a hydrogen distribution model developed by Coe and Chano to determine the amount of hydrogen present at the crack location at the time of fracture. The stress intensity and hydrogen content responsibile for the microvoid coalescence fracture mode have been quantified for the high strength steel used in this study. The resulting relationship agrees with the results of Beachem but extend his theory to a wider range of hydrogen contents.

U.S. Army Materials Technology Laboratory
Watertown, Massachusetts 02172-0001
ASSESSING HYDROGEN ASSISTED CRACKING MODES IN HIGH STRENGTH STEEL WELDS -
Steven A. Gedeon and Thomas W. Eagar

AD____________
UNCLASSIFIED
UNLIMITED DISTRIBUTION

Key Words

High strength steel
Welding
Implant tests

Technical Report MTL TR 88-44, December 1988, 13 pp-illus-tables, D/A Project 16162105.AH84, AMCMS Code 612105.H84

The stress intensity which causes crack propagation in high strength steel weldments was quantified as a function of the hydrogen content at the crack location. This relationship was used to assess previously proposed theoretical hydrogen assisted cracking mechanisms. It was found that the microplasticity theory of Beachem can best describe how the stress intensity factor and hydrogen content affect the modes of intergranular, quasi-cleavage, and microvoid coalescence fracture. Implant test results were analyzed with the aid of fracture mechanics to determine the stress intensity associated with various models of fracture. Diffusible weld hydrogen results were analyzed with the aid of a hydrogen distribution model developed by Coe and Chano to determine the amount of hydrogen present at the crack location at the time of fracture. The stress intensity and hydrogen content responsibile for the microvoid coalescence fracture mode have been quantified for the high strength steel used in this study. The resulting relationship agrees with the results of Beachem but extend his theory to a wider range of hydrogen contents.